Effect of Oxygen Stoichiometry on Microstructural and Magnetic Properties of FePt/TaO_x Bilayer Fabricated by Ion-Beam-Bombardment Deposition

G. J. Li[1], C. W. Leung[2], Y. C. Chen[3], J. H. Hsu[4], A. C. Sun[5], K. W. Lin[3], *Senior Member, IEEE*, and Philip W. T. Pong[1], *Senior Member, IEEE*

[1]Department of Electrical and Electronics Engineering, The University of Hong Kong, Hong Kong
[2]Department of Applied Physics, Hong Kong Polytechnic University, Hong Kong
[3]Department of Materials Science and Engineering, National Chung Hsing University, Taichung 402, Taiwan
[4]Department of Physics, National Taiwan University, Taipei 106, Taiwan
[5]Department of Chemical Engineering and Materials Science, Yuan Ze University, Chungli 32003, Taiwan

The effect of TaO_x capping layer on microstructures and magnetic properties of FePt thin films via annealing was studied. The structural ordering of FePt from face-centered cubic to face-centered tetragonal phases depends strongly on the oxygen contents in the capping TaO_x layer. The role of the TaO_x layer is used to separate the FePt grains, as revealed by TEM. The annealed FePt/TaO_x (15%O_2/Ar) exhibited the largest out-of-plane coercivity ($H_c \sim 4.2$ kOe) amongst all samples, compared to that ($\sim$2.4 kOe) in the reference FePt layer. At low oxygen content in FePt/TaO_x bilayers, the Ta atoms may act as defects to obstruct the FePt ordering whereas at high oxygen contents, the excess oxygen atoms diffuse into the FePt layer and react with Fe to form iron oxides which give rise to the low coercivities, as characterized by the XPS depth profile and binding energy analysis.

***Index Terms*—FePt, ion-beam bombardment, magnetic properties.**

I. Introduction

THE development of ultrahigh density recording media needs magnetic materials with high crystalline anisotropy such as $L1_0$ phase alloy, including FePt and CoPt [1]–[3]. FePt is a binary alloy and stoichiometry FePt has two phases at room temperature, soft magnetic face-centered cubic (fcc) phase and hard face-centered tetragonal (fct) phase. However, fct phase FePt cannot be directly synthesized and it can only be transformed from fcc phase FePt through annealing at temperatures higher than 580 °C [4]–[8].

Researchers have been working on improving the thin-film performance of FePt by adjusting microstructural and magnetic properties. Underlayer and capping layer are both known to influence the thin-film property by diffusion or grown seed-layer effect [9]–[14]. FePt with different underlayers has been widely investigated. By introducing a Bi underlayer, the transformation temperature can be lowered down to 300 °C [9]. With an Au/Cu underlayer, FePt annealed at 350 °C becomes ferromagnetic with coercivity up to 7.5 kOe [10]. Also, annealing at 300°C can provide FePt with 5.2 kOe in-plane coercivity using an AgCu underlayer [11]. Meanwhile, FePt thin film with different capping layers is also being investigated. Ag capped FePt showed stronger (001) orientation than the uncapped one [12]. FePt capped with amorphous SiO_2 can reduce intergrain coupling among FePt grains [13]. It was also found that by capping SiO_x layer on FePt, the grain size of FePt can be reduced by increasing the oxygen content in the capping SiO_x layer [14]. TaO_x is active in diffusion during annealing [15] so TaO_x has the potential to form grain boundaries for separating the FePt grains.

In this paper, FePt (10 nm) capped by TaO_x (10 nm) with different oxygen contents, ranging from 0% to 41%, was systemically investigated. The dependence of microstructural and magnetic properties on the oxygen content was studied.

II. Experiment

The FePt films (10 nm) were cosputtered first on SiO_2 substrates using an ultrahigh vacuum magnetron sputtering system with a substrate rotation speeds of 10 rpm [16]. Then the 10 nm capping TaO_x layer was grown on top of the FePt layer by the dual ion-beam deposition. A Kaufman source (800 V, 7.5 mA) was used to focus an Ar ion beam onto the Ta target surface while the End-Hall source ($V_{EH} = 100$ V) was used to in-situ bombard and clean the substrates during the Ta-oxide deposition with an oxygen content ranging from 0% to 41% O_2/Ar. Then the samples were annealed in vacuum at 550 °C for 10 min with no external magnetic field. The crystalline structures of the FePt/TaO_x bilayers were characterized by grazing angle x-ray diffraction using a Bruker D8 SSS diffractometer with a Cu Kα source. A JEOL JEM-2010 transmission electron microscopy (TEM) system operating at 200 kV was used for the structures, microstructures and grain sizes characterization. The magnetic properties of the as-deposited and annealed samples were measured with a Lake Shore-7407 vibrating sample magnetometer (VSM). An ULVAC-PHI X-ray Photoelectron spectroscope (XPS, PHI 5000 Versa Probe) was used for the depth profile analysis and to identify the oxidation states.

III. Results and Discussion

The FePt/TaO_x bilayers with different oxygen contents were annealed at 550 °C for 10 min and some of them exhibit fct phase FePt. This is evidenced by the (001), (111), (200), and (002) peaks of XRD spectra in Fig. 1. The annealed 15% O_2/Ar bilayer consisted of more ordered fct FePt structures. With

Manuscript received November 05, 2012; revised January 17, 2013; accepted February 08, 2013. Date of current version July 15, 2013. Corresponding authors: K.-W. Lin and P. W. T. Pong (e-mail: kwlin@dragon.nchu.edu.tw; ppong@eee.hku.hk).

Color versions of one or more of the figures in this paper are available online at http://ieeexplore.ieee.org.

Digital Object Identifier 10.1109/TMAG.2013.2247383

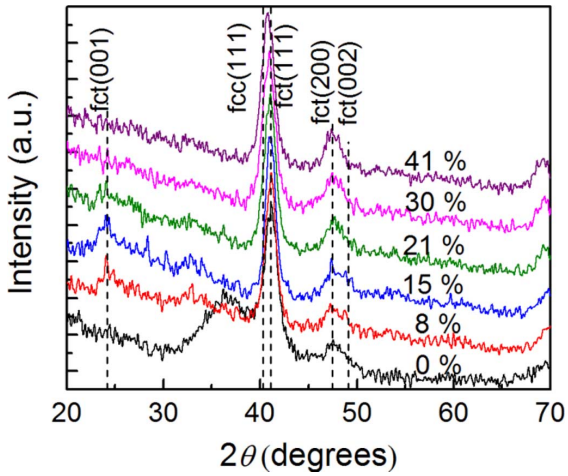

Fig. 1. XRD diffraction patterns of FePt/TaO_x with different oxygen contents (O_2/Ar) in TaO_x after annealing at 550°C for 10 min.

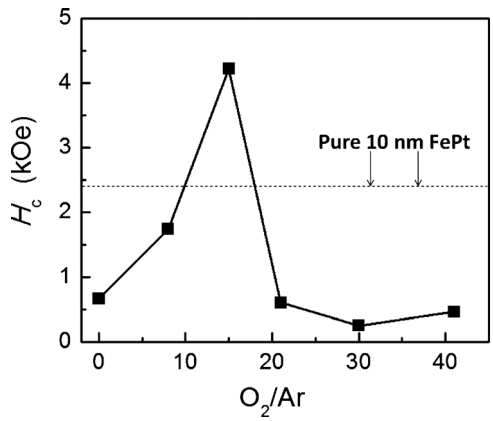

Fig. 2. Relation between out-of-plane coercivity and oxygen content in O_2/Ar for FePt/TaO_x bilayer after annealing at 550 °C for 10 min. As a reference, the coercivity of a 10 nm thick pure FePt in the perpendicular direction is 2.42 kOe.

higher amount of oxygen contents in Ta-oxide layers (e.g., 41% O_2/Ar), the vanish in the (001) orientation and the peak shift from fct to fcc (111) at 2-theta ~41° indicate excess oxygen may hinder FePt ordering.

The magnetic properties (H_c vs % O_2/Ar) of the annealed FePt/TaO_x bilayers are shown in Fig. 2. The coercivity in the out-of-plane direction for the pure FePt layer after annealing is $H_c \sim 2.4$ kOe. The annealed 15% O_2/Ar bilayer exhibits the largest coercivity (~4.2 kOe) amongst all samples. At low oxygen contents, the low H_c indicate the Ta atoms play important roles in obstruct FePt structural ordering from fcc to fct. On the other hand, the low coercivities in these annealed FePt/TaO_x bilayers with higher oxygen contents indicate that the interaction between Fe and O to form Fe-oxides is likely to occur and hinder the ordering transition, as compared to the coercivity in a pure reference FePt layer.

From the above results, we can observe that the oxygen content has remarkable influence on the crystalline structure of FePt after annealing. The coercivity which is correlated with the fct phase content can be enhanced by optimizing the oxygen content. Therefore, adjusting the oxygen content provides a possible route for improving the FePt coercivity.

In order to understand the effect of oxygen content on microstructure, high resolution TEM (HRTEM) was performed to analyze the sputtered FePt/TaO_x bilayers. It was found that by using a rotation speed of 10 rpm during the fabrication of Fe and Pt layers [16], the FePt would tend to form separated grain rather than plain thin films. The as-deposited FePt/TaO_x (0% O_2/Ar) bilayer is a grain-separated film with average grain size of 15.3 ± 2.9 nm as shown in Fig. 3(a). From the electron diffraction patterns in the inset of Fig. 3(a), fcc phase FePt can be identified by the fcc (222), (220), (200), and (111) peaks, and Ta can be identified by the bcc (110), (310), and (400) peaks. However, no peaks can be observed for fct phase FePt. As the oxygen content increased, the average grain size of the as-deposited FePt/TaO_x (15% O_2/Ar) bilayer decreased to 7.1 ± 1.4 nm in Fig. 3(b). Similar to the previous FePt/TaO_x (0% O_2/Ar) sample, fcc phase FePt is evidenced by the (111), (200), (220) and (222) peaks and Ta_2O_5 is proved by the Ta_2O_5 (4 15 1) peak in the inset of Fig. 3(b). As the oxygen content further increased to 41%, the average grain size increased to 8.5 ± 2.7 nm as measured from Fig. 3(c). Fcc FePt phases were observed in the electron diffraction patterns in the inset of Fig. 3(c). After the above samples were annealed at 550 °C for 10 min, their grain sizes changed. The separated FePt grains provide a fast-diffusion path for TaO_x during annealing; meanwhile, TaO_x exhibits insolubility and lower surface energy in FePt, so the top TaO_x layer would diffuse into FePt and form grain boundaries to separate the FePt grains after annealing. The grain size of the FePt-TaO_x (0% O_2/Ar) after annealing decreased to 9.9 ± 2.0 nm as shown in Fig. 3(d). The fct phase FePt was identified by the signature peaks including (110), (002), and (202) in the electron diffraction patterns (inset of Fig. 3(d)), indicating the phase transition from fcc to fct occurred due to annealing. As the oxygen content increased to 15%, the surface morphology became rough and the average grain size increased to 11.5 ± 2.5 nm as shown in Fig. 3(e). Fct phase FePt (001) signature peak was observed in the electron diffraction patterns [inset of Fig. 3(e)], indicating more fct phase FePt existed in the 15% O_2/Ar bilayer than the 0% O_2/Ar sample due to the increasing amounts of TaO_x incorporated into the bottom FePt layer as grain boundaries to separate the FePt grains during annealing. As the oxygen content further increased, the thin film surface consisted of grains with average size of 10.0 ± 2.3 nm in Fig. 3(f). No obvious (001) peak was identified in this oxygen content sample in the electron diffraction pattern [inset of Fig. 3(f)], indicating less fct phase existed than the 15% O_2/Ar one.

The above TEM results showed that the FePt/TaO_x (15% O_2/Ar) bilayer exhibited the largest grain-size and highest fct phase content after annealing at 550 °C for 10 min, which agrees with the XRD diffraction patterns results where the 15% Ar/O_2 sample exhibited the highest content of fct phase FePt. This signifies that the fct phase FePt content and thin film morphology of the FePt/TaO_x are both dependent on the oxygen content. However, further increasing the oxygen content exhibited adverse effect on fct FePt content and grain size. Thus the oxygen content must be optimized in order to boost up the grain growth and the fct FePt content.

The effect of the TaO_x capping layer on the microstructure of FePt is dependent on the oxygen content as observed from the above results. We may obtain further insight on this dependence by investigating the interdiffusion between the FePt and

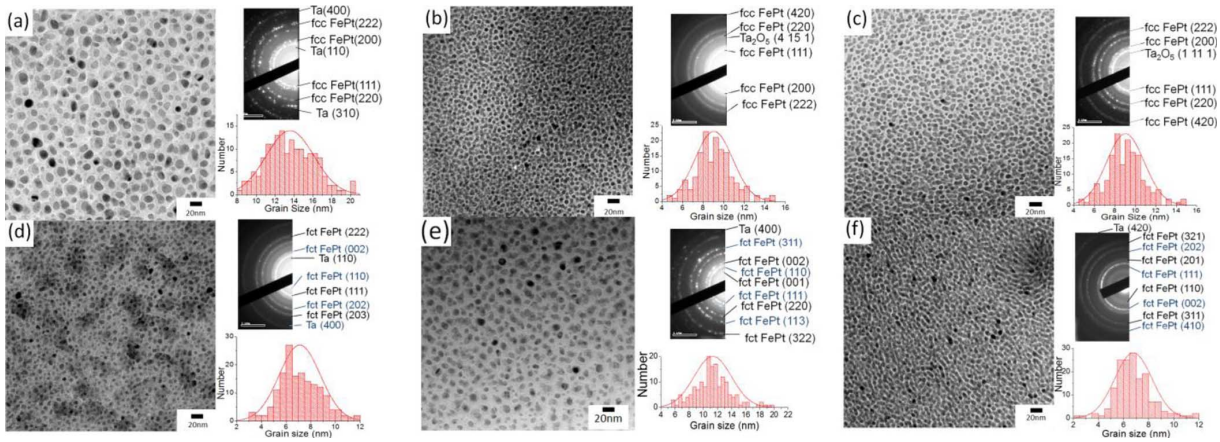

Fig. 3. HRTEM image and electron diffraction patterns of $FePt/TaO_x$ bilayer. The grain size distribution is measured and displayed for each sample. (a) As deposited 0% O_2/Ar. (b) As deposited 15% O_2/Ar. (c) As deposited 41% O_2/Ar. (d) 0% O_2/Ar after annealing at 550 °C for 10 min. (e) 15% O_2/Ar after annealing 550 °C for 10 min. (f) 41% O_2/Ar after annealing 550 °C for 10 min.

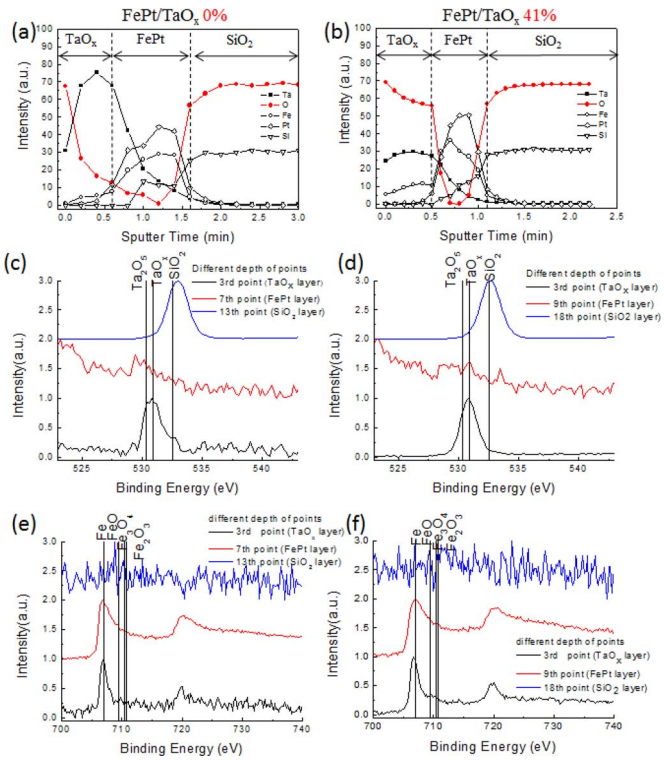

Fig. 4. XPS results for $FePt/TaO_x$ bilayers with different oxygen contents in O_2/Ar after annealing at 550° C for 10 min. (a) Depth profile for 0%. (b) Depth profile for 41%. (c) Binding energy of O 1s for 0%. (d) Binding energy of O 1s for 41%. (e) Binding energy of Fe 2p for 0%. (f) Binding energy of Fe 2p for 41%.

TaO_x layer after annealing at 550 °C for 10 min. X-ray photoelectron spectroscopic (XPS) characterization was performed and the XPS depth profiles as well as the corresponding XPS binding energies are shown in Fig. 4. Two transition regions are marked for the interfaces at TaO_x/FePt and $FePt/SiO_2$ for the 0% O_2/Ar sample at the sputter time of 0.6 and 1.6 min, respectively, as shown in Fig. 4(a). The two transition regions move left to 0.5–1.1 min for the sample with 41% O_2/Ar as shown in Fig. 4(b). The oxygen and iron binding energies are used to identify the metal-oxide types in the FePt layer in Fig. 4(c)–(f). The $Ta^{5/2}$ and Ta^{x+} ions peaks in XPS binding energy permit the identification of Ta_2O_5 and TaO_x. Fig. 4(c) clearly shows the Ta_2O_5 peak (530.3 eV) determining the Ta_2O_5 phase for films prepared with 0% O_2/Ar during the ion beam bombardment. The intensity of TaO_x is dominating in Fig. 4(d) when the O_2/Ar ratio is increased to 41% as evidenced by the TaO_x peak at 530.9 eV. In higher binding energies region ranging from 700 to 740 eV, the different Fe^{2+} and Fe^{3+} ions are used to identify FeO, Fe_2O_3 and Fe_3O_4 in the FePt layer besides the dominant Fe peak at 707 eV. The Fe^{2+} peak at 709.3 eV identifies the FeO existence in the FePt with 0% O_2/Ar after annealing in Fig. 4(e). Meanwhile, the Fe_2O_3 is identified with the weak Fe^{3+} peak at 710.8 eV in Fig. 4(f), indicating the existence of Fe_2O_3 in the FePt layer with 41% O_2/Ar after annealing. From the XPS depth profile analysis in Fig. 4(a) and (b), it is seen that the oxygen does not follow the same trend as Ta with increasing sputter time. This indicates that the detected oxygen signal has two sources in the FePt layer to affect the structure and magnetic properties. The drop and increased intensity in oxygen near the interface between TaO_x and FePt as well as between FePt and SiO_2 indicate the oxygen may react with Fe to form Fe-oxides (such as FeO, Fe_2O_3, and/or Fe_3O_4) after annealing, as revealed by the peaks of Fe 2p in Fig. 4(e) and (f). In addition, the high Si signal extends from SiO_2 layer into FePt layer indicate the formation of Fe silicide may occur due to annealing. This gives rise to the little fct FePt structures by XRD in Fig. 1 and explains low coercivities observed in Fig. 2. In both annealed 0% and 41% O_2/Ar bilayers, the strong peaks in O 1s ($\sim$533 eV) are characteristic of oxygen bonding to Si from the SiO_2 substrate, as shown in Fig. 4(c) and (d). However, the stronger O 1s peak ($\sim$531 eV) in the annealed 41% O_2/Ar bilayer than the noisy one in the annealed 0% O_2/Ar bilayer confirms the presence of the excess oxygen during depositing the capping Ta-oxide layer. The low O 1s signal in both samples [Fig. 4(c) and (d)] indicate that the oxygen may exist in the form of grain boundaries to separate the FePt grains, in agreement with the results obtained by TEM in Fig. 3. Further, the low coercivities in these annealed $FePt/TaO_x$ bilayers are attributed to the formation of Fe-oxides (such as FeO, Fe_2O_3 and Fe_3O_4), as identified in the Fe 2p peaks in Fig. 4(e) and (f), respectively.

The XPS depth-profile study shows that the TaO_x layer diffuses into the FePt layer and the diffusion depth varies with the oxygen content. Thus the microstructure changes with the oxygen content, which is attributed for the dependence of grain size on the oxygen content. Meanwhile, the oxygen atoms during the ion-beam bombardment process also play an important role in determining the magnetic properties of FePt. At no oxygen ratios (0% O_2/Ar), isolated decoupled FePt grains experienced less barrier during magnetization reversal processes and thus a small coercivity was observed. At higher oxygen ratios (8% and 15% O_2/Ar), the oxygen atoms might occupy the interstitial positions in the FePt lattice which may induce a local strain and thus enhance the FePt magnetic ordering. However, at even higher oxygen ratios (21%, 30%, and 41% O_2/Ar), the excess oxygen atoms were likely to react with Fe to form Fe-oxides and thus hinder the FePt ordering and give rise to the low coercivities.

IV. Conclusion

The structures, microstructural and magnetic properties of FePt/TaO_x bilayer were found to be dependent on the oxygen content in the capping TaO_x layer. The FePt grains separated by grain boundaries TaO_x have been achieved through annealing processes. While lower oxygen contents in the TaO_x layer may result in the Ta atoms act as defects and diffuse into the FePt lattice to hinder the FePt ordering, and higher oxygen contents is likely to cause the oxidation process between Fe and O to form iron oxides near TaO_x and FePt interfaces. The largest out-of-plane coercivity of 4.2 kOe was acquired in the FePt/TaO_x bilayer with 15% O_2/Ar, and this is even larger than the pure FePt thin film. Thus the oxygen content of TaO_x capping layer can adjust the microstructural and magnetic properties of FePt thin film, which provides a means for further enhancing the quality of FePt thin films.

Acknowledgment

This work was supported in part by the Seed Funding Program for Basic Research and Small Project Funding from the University of Hong Kong, the RGC-GRF grant (HKU 704911P), the University Grants Council of Hong Kong (Contract No. AoE/P-04/08), and ITF Tier 3 funding (ITS/112/12).

References

[1] K. Barmak, J. Kim, S. Shell, E. B. Svedberg, and J. K. Howard, "Calorimetric studies of the A1 to L1(0) transformation in FePt and CoPt thin films," *Appl. Phys. Lett.*, vol. 80, pp. 4268–4270, June 3, 2002.

[2] S. Jeong, Y. N. Hsu, D. E. Laughlin, and M. E. McHenry, "Magnetic properties of nanostructured CoPt and FePt thin films," *IEEE Trans. Magn.*, vol. 36, no. 5, pp. 2336–2338, Sep. 2000.

[3] S. Jeong, M. E. McHenry, and D. E. Laughlin, "Growth and characterization of L1(0) FePt and CoPt $\langle 001 \rangle$ textured polycrystalline thin films," *IEEE Trans. Magn.*, vol. 37, no. 4, pp. 1309–1311, Jul. 2001.

[4] K. Aimuta, K. Nishimura, S. Hashi, and M. Inoue, "Fabrication of L1(0)-FePt thin films by rapid thermal annealing," *IEEE Trans. Magn.*, vol. 41, no. 10, pp. 3898–3900, Oct. 2005.

[5] C. H. Park, J. G. Na, P. W. Jang, and S. R. Lee, "Effects of annealing condition on the structural and magnetic properties of FePt thin films," *IEEE Trans. Magn.*, vol. 35, no. 5, pp. 3034–3036, Sep. 1999.

[6] T. Seki, T. Shima, K. Yakushiji, K. Takanashi, G. Q. Li, and S. Ishio, "Improvement of hard magnetic properties in microfabricated L1(0)-FePt dot arrays upon post-annealing," *IEEE Trans. Magn.*, vol. 41, no. 10, pp. 3604–3606, Oct. 2005.

[7] J. S. Kim, Y. M. Koo, and N. Shin, "The effect of residual strain on (001) texture evolution in FePt thin film during postannealing," *J. Appl. Phys.*, vol. 100, no. 9, p. 093909, Nov. 1, 2006.

[8] N. Murayama, S. Soeya, Y. Takahashi, and M. Futamoto, "Ordering and grain growth of FePt thin films by annealing," *J. Magn. Magn. Mater.*, vol. 320, no. 3, pp. 3057–3059, Nov. 2008.

[9] C. Feng, B. H. Li, G. Han, J. Teng, Y. Jiang, Q. L. Liu, and G. H. Yu, "Low-temperature ordering and enhanced coercivity of L1(0)-FePt thin film promoted by a Bi underlayer," *Appl. Phys. Lett.*, vol. 88, no. 23, p. 232109, Jun. 5, 2006.

[10] Y. Zhu and J. W. Cai, "Low-temperature ordering of FePt thin films by a thin AuCu underlayer," *Appl. Phys. Lett.*, vol. 87, no. 3, p. 032504, Jul. 18, 2005.

[11] Y. S. Yu, H. B. Li, W. L. Li, M. Liu, and W. D. Fei, "Low-temperature ordering of L1(0) FePt phase in FePt thin film with AgCu underlayer," *J. Magn. Magn. Mater.*, vol. 320, no. 19, pp. L125–L128, Oct. 2008.

[12] J. L. Tsai, G. B. Lin, and H. T. Tzeng, "Magnetic properties and microstructure of (001) oriented Ag/FePt, Ag/FePt/Ag films," *J. Alloy. Compound*, vol. 487, no. 1–2, pp. 18–23, Nov. 13, 2009.

[13] Y. Ding, D. H. Wei, and Y. D. Yao, "Magnetic properties and microstructure of Fe/Pt multilayer films capped with SiO2 amorphous layer for magnetic recording use," *J. Appl. Phys.*, vol. 103, no. 7, p. 07E145, Apr. 1, 2008.

[14] K. W. Lin, Y. L. Chiu, A. C. Sun, J. H. Hsu, J. van Lierop, and T. Suzuki, "Ion-beam bombarded SiO_2 layer effects on the microstructure and magnetism in FePt/SiO2 bilayers," *Jpn. J. Appl. Phys.*, vol. 48, no. 7, p. 073002, Jul. 2009.

[15] P. Alen, M. Vehkamaki, M. Ritala, and M. Leskela, "Diffusion barrier properties of atomic layer deposited ultrathin Ta_2O_5 and TiO_2 films," *J. Electrochem. Soc.*, vol. 153, no. 4, pp. G304–G308, 2006.

[16] A. C. Sun, H. F. Hsu, Y. J. Wu, Y. L. Chiu, J. H. Hsu, P. W. T. Pong, T. Suzuki, and K. W. Lin, "Microstructures and magnetism of different oxides separating FePt grains via ion-beam bombardment and annealing," *Jpn. J. Appl. Phys.*, vol. 49, no. 12, p. 123001, Dec. 20, 2010.